Experimental evidence for subshell closure in ^{8}He and indication of a resonant state in ^{7}He below 1 MeV

F. Skaza, V. Lapoux, N. Keeley, N. Alamanos, E. C. Pollacco, F. Auger, A. Drouart, A. Gillibert, D. Beaumel, E. Becheva, et al.

▶ **To cite this version:**

F. Skaza, V. Lapoux, N. Keeley, N. Alamanos, E. C. Pollacco, et al.. Experimental evidence for subshell closure in ^{8}He and indication of a resonant state in ^{7}He below 1 MeV. Physical Review C, 2006, 73, pp.044301. 10.1103/PhysRevC.73.044301 . in2p3-00025918

HAL Id: in2p3-00025918
https://hal.in2p3.fr/in2p3-00025918

Submitted on 21 Dec 2006

HAL is a multi-disciplinary open access archive for the deposit and dissemination of scientific research documents, whether they are published or not. The documents may come from teaching and research institutions in France or abroad, or from public or private research centers.

L'archive ouverte pluridisciplinaire **HAL**, est destinée au dépôt et à la diffusion de documents scientifiques de niveau recherche, publiés ou non, émanant des établissements d'enseignement et de recherche français ou étrangers, des laboratoires publics ou privés.

Experimental evidence for sub-shell closure in ^{8}He and indication of a resonant state in ^{7}He below 1 MeV

F. Skaza[1], V. Lapoux[1],* N. Keeley[1], N. Alamanos[1], E.C. Pollacco[1], F. Auger[1], A. Drouart[1], A. Gillibert[1], D. Beaumel[2], E. Becheva[2], Y. Blumenfeld[2], F. Delaunay[2], L. Giot[3], K.W. Kemper[4], L. Nalpas[1], A. Obertelli[1], A. Pakou[5], R. Raabe[1],† P. Roussel-Chomaz[3], J-L. Sida[1], J.-A. Scarpaci[2], S. Stepantsov[6], and R. Wolski[7]

[1] *CEA-SACLAY DSM/DAPNIA/SPhN F-91191 Gif-sur-Yvette, France*
[2] *Institut de Physique Nucléaire, IN_2P_3-CNRS, F-91406 Orsay, France*
[3] *GANIL, Bld Henri Becquerel, BP 5027, F-14021 Caen Cedex, France*
[4] *Department of Physics, Florida State University, Tallahassee, Florida 32306-4350, USA*
[5] *Department of Physics, University of Ioannina, 45110 Ioannina, Greece*
[6] *JINR, FLNR 141980 Dubna, Moscow region, Russia and*
[7] *The Henryk Niewodniczanski Institute of Nuclear Physics, Krakow, Poland*

(Dated: March 21, 2006)

The spectroscopy of the unstable ^{8}He and unbound ^{7}He nuclei is investigated via the p(^{8}He,d) transfer reaction with a 15.7A.MeV ^{8}He beam from the SPIRAL facility. The emitted deuterons were detected by the telescope array MUST. The results are analyzed within the coupled-channels Born approximation framework, and a spectroscopic factor $C^2S = 4.4\pm1.3$ for neutron pickup to the ^{7}He$_{g.s}$ is deduced. This value is consistent with a full p3/2 subshell for ^{8}He. Tentative evidence for the first excited state of ^{7}He is found at E* = 0.9±0.5 MeV (width $\Gamma = 1.0 \pm 0.9$ MeV). The second one is observed at a position compatible with previous measurements, E*=2.9±0.1 MeV. Both are in agreement with previous separate measurements. The reproduction of the first excited state below 1 MeV would be a challenge for the most sophisticated nuclear theories.

PACS numbers: 25.60.-t,21.10.-k,21.10.Jx, 24.10.Eq

I. INTRODUCTION

The binding and excitation energies of the light weakly-bound neutron-rich nuclei are crucial benchmarks for microscopic models. In particular, since the dripline nucleus ^{8}He has the highest N/Z amongst the bound nuclei, its spectroscopy can help to clarify the isospin-dependent term in the most recent microscopic calculations. The theoretical description of ^{8}He seems possible either within the framework of microscopic cluster models (resonating group model RGM [1], cluster shell model [2]) or a large-basis no-core shell model (NCSM) space [3]. In the cluster models, the structure of ^{8}He is described as an alpha core surrounded by 4 neutrons, which constitute a skin or halo. Alternatively, the ground state (gs) of ^{8}He may be described as a mixing of the following configurations : ^{6}He(2^+)+2n and ^{6}He(0^+)+2n [4]. In the simple shell model (SM) picture, the gs of ^{8}He corresponds to a closed 0p3/2 shell, giving a sum rule estimate of the spectroscopic factor (SF) of $C^2S = 4.0$ for pickup of a neutron to the gs of ^{7}He. In order to test whether these pictures hold for ^{8}He, we have chosen the (p,d) reaction as a natural spectroscopic tool, also allowing the spectroscopy of ^{7}He to be investigated.

^{7}He is a particle unstable nucleus previously observed at Riken using the p(^{8}He,d) reaction at 50A.MeV [5]. In this pioneering work, the excitation spectrum for ^{7}He was deduced, with a low-lying resonant excited state at 3.3(3) MeV above the ^{6}He+n 0.44 MeV threshold being observed (E*=2.9 MeV, width Γ = 2.2(3) MeV). This excited state, which mainly decays into α+3n, was interpreted as a p1/2 neutron coupled to the ^{6}He core in its unbound 2^+ excited state, and a tentative spin assignment of $5/2^-$ was made [5]. This resonance was also observed at E*=2.95(10) MeV (Γ = 1.9(3) MeV), in the ^{9}Be(^{15}N,^{17}F)^{7}He reaction [6]. In the break-up experiment [7] with a ^{8}He beam on a Carbon target, the relative energy of the ^{6}He and neutron fragments was reconstructed and the fitted spectrum supported the assumption of a resonant state at E* = 0.6(1) MeV (Γ = 0.75(8) MeV). Based on the observation of the ^{6}He fragment, thus excluding the $5/2^-$ configuration associated to the unbound ^{6}He(2^+) core, it was discussed as a possible $1/2^-$ state [7]. Recently however, the low-lying excited states of ^{7}He were studied via the isobaric analog states (IAS) of ^{7}Li [8]. The authors do not confirm the above result, while they report that the analog of a very broad resonance ($1/2^-$,T=3/2) is located at an excitation energy above 2.2 MeV in ^{7}He. From the theoretical point of view, recent calculations [1, 3, 9] agree in predicting at least 2 resonances, $1/2^-$ and $5/2^-$, above the $3/2^-$ gs. Microscopic models do not predict any positive parity states at low energy. In the RGM [1], the $1/2^-$ and $5/2^-$ states are given by the coupling of a 0p1/2 neutron to the ^{6}He core, in its gs or 2^+ excited state, respectively. We present here the ^{8}He(p,d) reaction performed at 15.7A.MeV with better energy resolution and larger angular coverage than previously. The deduced ex-

*E-mail address: vlapoux@cea.fr
†permanent address: IKS, University of Leuven, B-3001 Leuven, Belgium

citation spectrum for ^{7}He is discussed together with the analysis of the differential distributions p(^{8}He,d)^{7}He$_{g.s}$ and p(^{8}He,d)^{7}He*. It should be noted that the $1/2^-$ and $5/2^-$ excited states were not observed simultaneously in previous experiments due to the experimental resolution or the selectivity of the observation process.

II. EXPERIMENTAL SET-UP AND ANALYSIS OF THE EXCITATION SPECTRA

The ^{8}He beam impinged on a proton target and the direct reactions were studied by detecting the light recoil. We adopted the same techniques as for the ^{6}He(p,p') experiment presented in [10]. The ^{8}He beam was produced by the ISOL technique and accelerated to 15.7A.MeV by the CIME cyclotron at the SPIRAL facility [11], with no contaminants. The maximum (average) intensity in the experiment was 14000 (5000) p/s. The proton target was a 8.25 mg/cm^2 thick polypropylene $(CH_2)_n$ foil. The beam profile and incident angle on the target were monitored event by event by two low-pressure multi-wire beam tracking detectors, CATS [12], located upstream of the target. The whole set-up is shown in Fig.1. The

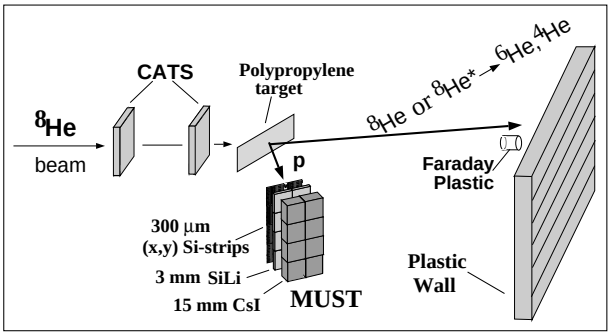

FIG. 1: Experimental set-up. The MUST array was assembled in a wall configuration, located 15 cm from the target. It was placed in 2 positions with the vertical axis rotated by an angle of 50° and 65° with respect to the beam axis in the laboratory frame.

MUST detector [13], an array of 8 three-stage telescopes, detected the recoil deuteron in coincidence with a wall of plastic scintillators measuring the projectile remnant. One module consisted of a 6x6 cm^2 x-y position sensitive Si-strip detector ($300\mu m$) backed with a Si(Li) (3 mm) and a CsI scintillator. Each strip detector had a minimum energy threshold of 0.5 MeV with angular and energy resolutions of 0.4° and 50 keV. Proton, deuteron and triton particles were identified at energies below 6, 8 and 9 MeV, respectively via the correlation between the time-of-flight (TOF) and the energy deposited in the Si-strip stage. For higher energies, the standard ΔE-E technique was applied. The beam and reaction fragments were detected in the forward direction either in a small plastic scintillator at zero degrees or for larger center of mass (c.m.) angles in the plastic wall covering an area of 50x48 cm^2 at 75.5 cm from the target. The wall gave time and energy measurements resulting in mass resolution δM/M $\simeq$ 19%, sufficient to identify roughly ^{8}He nuclei and substract background in the plastic signals, but not to discriminate ^{6}He from ^{8}He or from ^{4}He. The kinematics of the total energy of the light particle with respect to the scattering angle in the laboratory frame are plotted in Fig. 2a) and b), for events including a proton or a deuteron detected in MUST in coincidence with He isotopes in the plastic wall, respectively. From the proton or deuteron identification and with the kinematical plots of the reaction of interest elastic, inelastic (p,p') or (p,d) were selected. The elastic data extend from 20 to 110°$_{c.m.}$, the transfer data from 27 to 85°$_{c.m.}$. The total number of incident ^{8}He particles on the $(CH_2)_n$ target was 8.17 10^8. The excitation spectrum for ^{8}He and the differential cross sections for ^{8}He(p,p') will be presented in a forthcoming article. The excitation energy spectrum for ^{7}He was calculated by the missing mass method from the measured energy and angle of the scattered deuteron. First, the excitation spectrum was constructed by considering the whole statistics for the p(^{8}He,d) reaction, retaining only few events associated to small gates. These gates were chosen to exclude ^{4}He or ^{6}He thus allowing a strict identification of the ^{6}He (gate denoted "a") or ^{4}He (gate "b") in the plastic wall as shown by Fig. 3. The whole statistics, for all c.m. angles, were considered to discuss qualitatively the ^{7}He spectrum respected to the ^{6}He and ^{4}He fragments. Afterwards, for the quantitative discussion of the ^{7}He spectrum, we will consider thin c.m. slices in the (p,d) kinematics. We will need to consider a larger gate (noted "c") in order to have more statistics in the ^{7}He spectrum. Even if the discrimination between the ^{4}He and ^{6}He fragments is not achieved, having the deuteron in coincidence with either an ^{6}He or ^{4}He fragment will be enough in the second step.

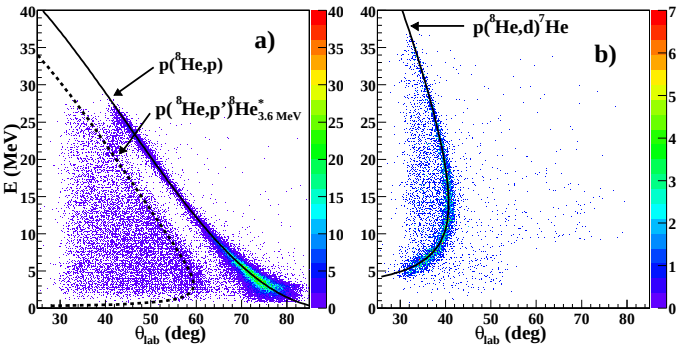

FIG. 2: Kinematical plot of events for : a) the ^{8}He elastic, inelastic reactions on protons and b) (p,d) transfer. The calculated lines of the reactions are drawn to guide the eye, the dashed line in a) represents the (p,p') to an excited state at 3.6 MeV.

First, the resulting excitation spectra for ^{7}He, associated to gates a and b are displayed in Fig. 4a. and 4b, respectively. The energies are referred to the gs of ^{7}He found at 0.44 MeV above the ^{6}He+n threshold [5]. Below

the ^{6}He(2^+)+n threshold (at E*=1.36 MeV compared to ^{7}He gs), a peak corresponding mainly to the ^{7}He gs is observed. Above the ^{4}He + 3n threshold (at 0.535 MeV), a broad resonance is observed (Fig. 4b) at E*= 2.9(1) MeV with a width Γ = 2.1(8) MeV. These parameters are in agreement with the values found in [5, 6]. The ratio, 0.6±0.3, between ^{4}He and total yields is also compatible with the previously measured branching ratio $\Gamma_{\alpha+3n}/\Gamma_{tot}$ =0.7±0.2 [5]. Following the theoretical indication of [1], the resonances observed mainly in coincidence with ^{6}He or ^{4}He would be attributed to $3/2^-$ gs and $5/2^-$ excited state, respectively.

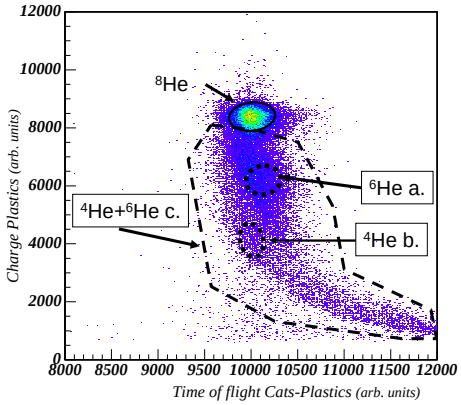

FIG. 3: Correlation spectrum of the charge in the plastic wall versus TOF. The data correspond to the events of ^{8}He on proton, for which a light charged particle (p,d, or triton) was detected in MUST. TOF is between the 2^{nd} beam detector CATS and the plastics. The contours (gates) indicated in the plot are discussed in the text.

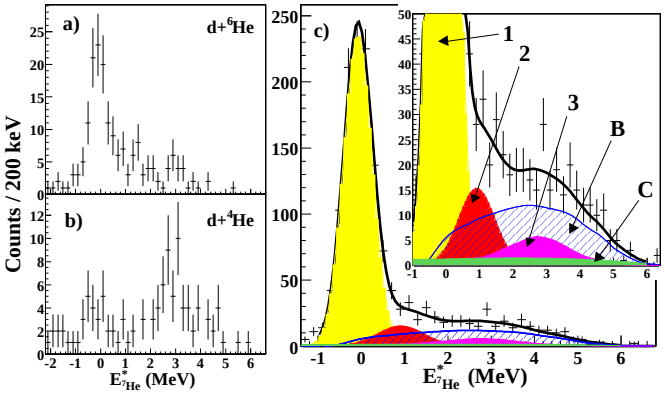

FIG. 4: Excitation spectra for ^{7}He with following conditions (see also the text) : a) coincidence with the deuteron and the ^{6}He fragment in the plastic wall ; b) coincidence with the ^{4}He ; c) the area 1 and 2, 3, B and C correspond to the resonances for the gs and 2 excited states, to the physical and Carbon backgrounds, respectively. The thick solid curve is the total fit including all contributions. The error bars on the points are statistical errors. The insert shows a zoom.

As a second step, to extract the characteristics of the possible resonances, we selected a thin angular slice where the energy straggling can be controlled. The (p,d) reaction was only selected by requiring the deuteron in coincidence with a He fragment (either ^{4}He or ^{6}He, as shown in gate "c" of Fig 3).

We constructed the ^{7}He excitation energy spectrum for angles between 50 and $60^\circ_{c.m.}$, where the FWHM resolution in excitation energy is δE^* = 590 (14) keV. The corresponding spectrum is presented as points in Fig. 4.c. The shape of the continuum background contribution to this spectrum is given by the area B. It was determined by a Monte-Carlo simulation of the physical background produced by few-body kinematics with several decay channels, and filtered by the experimental response. The ingredients of the simulation were the phase space calculations of the reaction channels, the detection efficiency and angular acceptance of the telescopes and plastic wall, and the experimental angular and energy resolutions.

The various reaction channels included in the simulation of the physical background are enumerated below, and their associated excitation energy spectra are plotted in Fig. 5. The few-body components are coming from :

• 3-body phase space, with channels :
^{8}He+p → d+n+^{6}He(0^+) (curve 1);
^{8}He+p → d+^{6}He(2^+)+n (curve 2);
^{8}He+p → d+^{5}He+ ^{2}n, with interaction in the final state between ^{4}He and one neutron and between the two remaining neutrons (curve 3);

• 4-body phase space,
^{8}He+p → d+^{4}He+^{2}n+n interaction in the final state between 2 amongst the 3 neutrons (curve 4);
^{8}He+p → d+^{5}He+n+n interaction in the final state between ^{4}He and one neutron (curve 5);

• 5-body phase space,
^{8}He+p → d+^{4}He+n+n+n (curve 6);

• 3-body phase space, with interaction in the final state between the 3 neutrons, ^{8}He+p → d+^{4}He+^{3}n (curve 7).

The notation ^in means that in the calculation the i neutrons were considered as correlated in the space framework. The channels producing the same kind of background were fitted by a common distribution. The relative contribution of each channel was arbitrary, and in test calculations each of them was considered alternatively as the main one to check the region in excitation energy in which they might contribute mostly. Our knowledge of the microscopic structure of ^{8}He did not allow to fix unambiguously the components of the physical background produced by the phase space. But several constraints could be applied to the resulting background curve. The overall normalization was left free and determined in order to superimpose the simulated excitation energy distribution with the measured one. The simulated shape (decrease and cuts) of the excitation energy spectrum in the energy region above 5 MeV was in agreement with the data, showing that all the experimental effects (angular acceptance, cuts) were well taken into

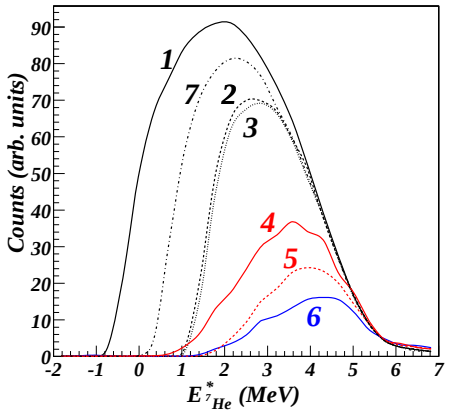

FIG. 5: Physical background contributions expressed as a function of the excitation energy for ^{7}He. Each curve is obtained by simulation of the various reaction channels detailed in the text.

account.

The background from the Carbon in the target (area C), was estimated by measuring the reactions of ^{8}He (number of incident particles being 1.8 10^8) on a Carbon target. The data were fitted with the continuum background contribution (area B), the Carbon component, and either one (the gs), 2 (gs and resonance at 2.9 MeV) or 3 resonances. The purpose was to check if our data could support the ^{7}He resonant state obtained by Meister et al. [7] below 1 MeV.

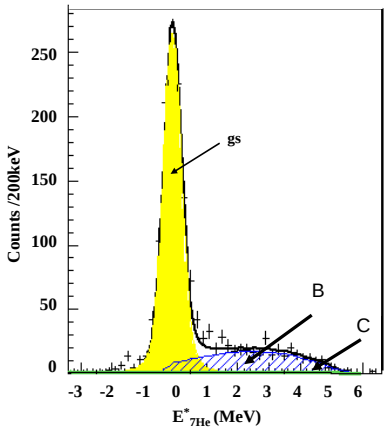

FIG. 6: Excitation spectrum for ^{7}He. Area B and C correspond to the physical and Carbon backgrounds, respectively. The thick solid curve is the total fit including gs resonance and all contributions. The error bars on the points are statistical errors.

In the angular range between $50_{c.m.}$ and $60_{c.m}$, the χ_2/N value for the 2-peak fit was 1.5, for the 3-peak fit it was 0.96. The total curve for the 2-peak fit (no 1 MeV resonance included) is shown for comparison in Fig. 6. For each angular slice taken into account the same features for the resonances were found and a better χ_2 was obtained when including the 3 resonances rather than with the 2-peak fit. The result of the best fit obtained with 5 components including 3 resonances is shown in Fig. 4.c. During the fitting procedure, Breit-Wigner (BW) functions folded with the experimental resolution were adopted to describe the gs (area 1) and the resonances (area 2,3). The 2^{nd} excited state, being embedded in the background, was described with position and width of the BW function fixed to previous values : 2.9 MeV and Γ = 2.1 MeV respectively. The parameters of the gs and the 1^{st} excited state were left free together with the normalization of the continuum background. The components corresponding to the best fit and total curve are presented in Fig. 4.c. The position of the resonances was found to be independent of angle for various angular slices, which confirms the existence of nuclear states. The resonance curves were unfolded with a Gaussian function to subtract the experimental resolution and are given as BW functions. The gs is located at 0.36(5) MeV above the ^{6}He + n threshold, with width Γ = 0.17(5) MeV.

Even if the resonance cannot be extracted with enough statistics, it is not excluded by our data, and we can indicate this 1^{st} excited state at E* = 0.9(5) MeV (1.3 MeV above threshold) with width Γ = 1.0(9) MeV, which is consistent with the results obtained in [7]. It is in contrast with the conclusions from [8] based on the observation of the IAS of ^{7}He in ^{7}Li. Although the background under the 1^{st} excited state is large, it is important to stress that no physical decay mode was found to be able to produce directly a significant contribution in the region of 1 MeV. It was checked that, when the contribution of a specific reaction channel was enhanced to produce an amount of counts around 1 MeV, then the agreement of the total curve with the data points at higher energies was less good, showing that the excess of counts observed around 1 MeV is rather due to a resonance than to a background effect.

III. ANALYSIS OF THE TRANSFER CROSS SECTIONS

We now discuss the differential cross sections extracted from our data. Including statistical and systematic errors, the normalization of the data for elastic scattering and transfer to the ^{7}He gs has a total uncertainty of $\simeq$ 15 %, mainly from the subtraction of the background, the acceptance of the detection system (±5%), the target thickness (±5%) and the efficiency in the detection of the incident ^{8}He (±2%).

In order to obtain a SF for neutron pickup to the ^{7}He$_{gs}$ from the p(^{8}He,d) data, a series of coupled-channels Born approximation (CCBA) calculations was carried out using the code Fresco [14]. This analysis requires a p+nucleus potential in the entrance and a d+nucleus po-

tential in the exit channel. The bare d+nucleus potential was the Watanabe type [15], generated by single-folding of proton, neutron + nucleus potentials. Couplings to the deuteron breakup were included in the exit channel using the continuum-discretized coupled-channels (CDCC) formalism, as described in [16] and the transfer step was treated within the usual prior-form distorted-wave Born approximation (DWBA). The calculated p(^{8}He,d) distributions for angles smaller than $\simeq 30^\circ_{c.m.}$, used to define the SF, were found to be essentially independent of the choice of entrance potential. This potential was taken from the CH89 parameterization [17] modified to fit to the measured elastic scattering data. In order to test the

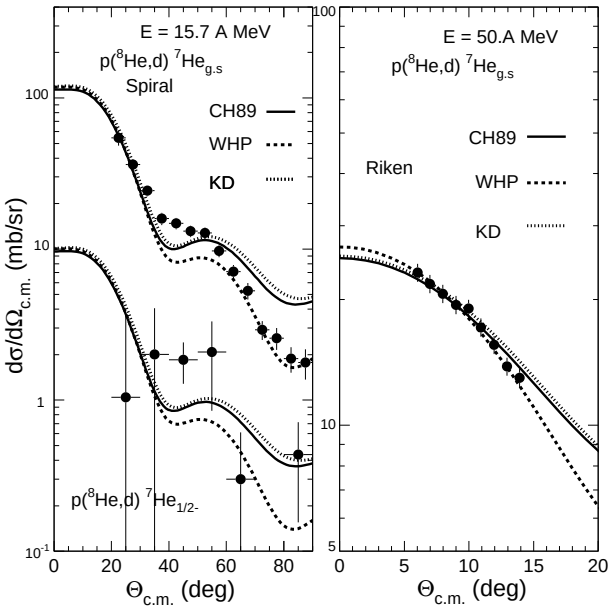

FIG. 7: Analysis of the (p,d) cross sections to ^{7}He$_{g.s}$ and ^{7}He$_{1/2-}$ obtained at 15.7 and (p,d)^{7}He$_{g.s}$ at 50A.MeV [5].

sensitivity of our results to the choice of n,p+^{7}He potentials, a series of calculations using various global nucleon optical potential systematics was performed. We present results for 3 sets : CH89 for both n and p, Koning and Delaroche (KD) [18] for both neutron and proton, Wilmore and Hodgson [19] for neutron and Perey [20] for proton (WHP). The neutron binding potential for the p/d overlap was given by the Reid soft-core interaction [21], including the small D-state component of the deuteron gs. For the ^{8}He/^{7}He overlap we used standard values of $R_0 = ro \times A^{1/3}$ fm with $ro = 1.25$ fm and $a = 0.65$ fm. The ^{8}He(p,d) transfer data at 15.7A.MeV are presented in Fig.7 together with the data obtained at 50A.MeV at Riken [5]. The dashed, dotted and solid curves show the cross sections obtained with the WHP, KD, CH89 potentials respectively. At 15.7A.MeV, the best fit C^2S value obtained for each set of potentials corresponds to 4.4 ; at 50A.MeV the C^2S values range from 4.0 (KD), to 4.4 (CH89) and 4.6 (WHP). For a given choice of exit potentials, varying the n+^{7}He binding potential radius between $ro = 1.0$ and 1.5 fm was found to lead to variations of up to 20 % in the extracted SF. We therefore obtain a value of $C^2S = 4.4 \pm 1.3$, taking into account all sources of uncertainty. The cross section for transfer to the 0.9 MeV resonance is compatible with an L=1 calculation (spin $1/2^-$ or $3/2^-$) and upper limit deduced for the SF is 0.2. Combined with the observation of the ^{6}He fragment, the spin assignment of the resonance found at low energy 0.9(5) MeV is consistent with a $1/2^-$. The characteristics of the ^{7}He resonances obtained in previous experiments are summarized and compared to microscopic calculations in Fig. 8.

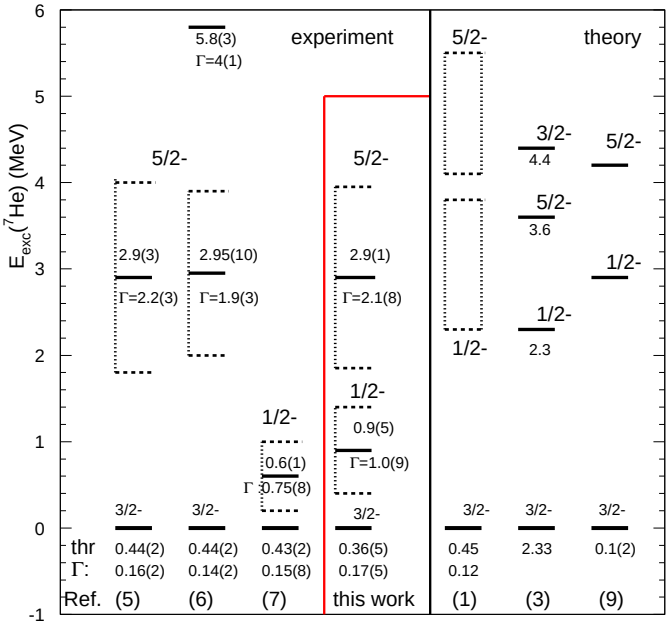

FIG. 8: Experimental and theoretical spectra of ^{7}He. The threshold energy indicated for the models is deduced from the predicted binding energy for ^{7}He and the energies of the excited states are given with respect to the calculated gs.

Recent predictions of the $1/2^-$ energy given by large basis NCSM [3] and Quantum Monte-Carlo (QMC) calculations [9] are 2.3 and 2.9 MeV, respectively. Note that in Ref. [3] the ^{7}He gs is found 2 MeV higher than the experimental value. In the QMC the agreement is better but the $5/2^-$ is predicted 1.3 MeV higher. In the RGM [1] the predicted resonant energies are between 2.3-3.8 MeV but could be even lower depending on the assumptions made on the $1/2^-$ resonance.

IV. CONCLUSIONS

In the search for the predicted $1/2^-$ 1^{st} excited state, Golovkov et al. [22] studied the d(^{6}He,p)^{7}He reaction; no resonance was found above the gs. But it should be noted that a better microscopic description of the nuclear structure and reactions embedded in the continuum is required in order to understand the measured positions and widths of the excited resonances given by separate experiments. Recently, within the recoil corrected continuum SM calculations [23], the conclusion in [8] was found premature. From our work, combined with the conclusions underlined in [23] about the structure of ^{7}He($1/2^-$), this state could be conceived as more complicated than a simple mixing of ^{6}He(0^+)+n and ^{6}He(2^+)+n configurations. Therefore, these features might not be incompatible : being not simply built on ^{6}He(0^+), ^{7}He($1/2^-$) is not seen in ^{6}He(d,p) but seen in break-up experiment of ^{8}He ; it is indicated here in ^{8}He(p,d), and weakly populated due to its small SF to ^{8}He(0^+). If the observations for the 3 resonant states are confirmed, and compatible with the following quantum numbers : $3/2^-$, $1/2^-$, $5/2^-$, this sequence would then be in agreement with a simple SM picture, and well understood in most of the microscopic models. However, the excitation energies are predicted higher than found experimentally. From our results, we can indicate that the ^{8}He(p,d) reaction is the best one for a tentative measurement of the first excited state in ^{7}He. Combining good ^{4,6,8}He separation as in [5] and energy resolution with our present technique would help in clarifying the characteristics of this state.

In conclusion, from the ^{8}He(p,d)^{7}He reaction, we have observed the ^{7}He gs, the excited state around 3 MeV, and have indication for the 1^{st} excited state below 1 MeV. We have obtained a value for C^2S supporting a relatively pure $(p3/2)^4_\nu$ configuration for the ^{8}He gs.

Acknowledgments

The help of P. Gangnant, J.-F. Libin (GANIL), L. Petizon and M. Vilmay (IPN-Orsay), during the preparation of the experiment, is gratefully acknowledged.

[1] J. Wurzer and H.M. Hofmann, Phys. Rev. C **55**, 688 (1997).
[2] M.V. Zhukov, A.A. Korsheninnikov, and M.H. Smelberg, Phys. Rev. C **50** R1 (1994).
[3] P. Navràtil and B.R. Barrett, Phys. Rev. C **57**, 3119 (1998).
[4] A.A. Korsheninnikov *et al.*, Phys. Rev. Lett. **90**, 082501 (2003).
[5] A.A. Korsheninnikov *et al.*, Phys. Rev. Lett. **82**, 3581 (1999).
[6] H.G. Bohlen et al., Phys. Rev. C **64**, 024312 (2001).
[7] M. Meister et al., Phys. Rev. Lett. **88**, 102501 (2002).
[8] G. V. Rogachev *et al.*, Phys. Rev. Lett. **92**, 232502 (2004).
[9] S.C. Pieper, V.R. Pandharipande, R.B. Wiringa, and J. Carlson, Phys. Rev. C **64**, 014001 (2001).
[10] A. Lagoyannis *et al.*, Phys. Lett. B **518**, 27 (2001).
[11] A. C. Villari *et al.*, Nucl. Phys. **A693**, 465 (2001).
[12] S. Ottini *et al.*, Nucl. Instrum. Methods Phys. Res. A **431**, 476 (1999).
[13] Y. Blumenfeld *et al.*, Nucl. Instrum. Methods Phys. Res. A **421**, 471 (1999).
[14] I. J. Thompson, Comput. Phys. Rep. **7**, 167 (1988).
[15] S. Watanabe, Nucl. Phys. **8** (1958) 484.
[16] N. Keeley, N. Alamanos, and V. Lapoux, Phys. Rev. C **69**, 064604 (2004).
[17] R.L. Varner, W.J. Thompson, T.L. McAbee, E.J. Ludwig, and T.B. Clegg, Phys. Rep. **201**, 57 (1991).
[18] A.J. Koning and J.P. Delaroche, Nucl. Phys. **A713**, 231 (2003).
[19] D.Wilmore and P.E.Hodgson, Nucl. Phys. **55**, 673 (1964).
[20] F.G. Perey, Phys. Rev. **131**, 745 (1963).
[21] R.V. Reid, Jr., Ann. Phys. (N.Y.) **50**, 441 (1968).
[22] M.S. Golovkov et al., Physics of Atomic Nuclei **64**, 1244 (2001).
[23] D. Halderson, Phys. Rev. C **70**, 041603(R) (2004).